JOURNAL OF SOLID STATE CHEMISTRY 7, 468–473 (1973)

Luminescence of Mn^{2+} in $SrGa_{12}O_{19}$, $LaMgGa_{11}O_{19}$, and $BaGa_{12}O_{19}$

J. M. P. J. VERSTEGEN

N.V. Philips' Gloeilampenfabrieken, Eindhoven, The Netherlands

Received October 31, 1972

Lattice parameters are given of $SrGa_{12}O_{19}$, $BaGa_{12}O_{19}$, and $LaMgGa_{11}O_{19}$, three new gallates with the magnetoplumbite structure. The luminescence of the compounds without and with activation by Mn^{2+} is reported. The quantum efficiencies of the Mn^{2+} phosphors are between 15% ($BaGa_{12}O_{19}$:Mn) and 70% ($\{Sr_{1-x}La_x\}Ga_{12-x}Mg_xO_{19}$:Mn). The emission strongly resembles that of Mn^{2+} in $MgGa_2O_4$. The fine structure of the Mn^{2+} emission band at 77°K is due to phonon coupling.

Introduction

Cathodoluminescence of Mn^{2+}-activated aluminates is a familiar phenomenon reported by Kröger in respect of $MgAl_2O_4$, $ZnAl_2O_4$, $MO \cdot 6\ Al_2O_3$ (M = Ca, Sr, Ba), and $A_2O \cdot 11\ Al_2O_3$ (A = Na, K) (1). Substitution of Ga for Al in the spinels ($MgAl_2O_4$, $ZnAl_2O_4$) causes the Mn^{2+} phosphors to luminesce under 254 nm radiation (*2*, *3*). The present work deals with the Ga derivatives having the magnetoplumbite structure ($MO \cdot 6\ Al_2O_3$), leading to three new compounds that, after activation with Mn^{2+}, showed narrow band green luminescence, strongly resembling that of Mn^{2+} in the spinels $MgGa_2O_4$ and $ZnGa_2O_4$.

Experimental

Phosphors were fired in stoichiometric proportions, the components being luminescent grade $CaCO_3$, $SrCO_3$, $BaCO_3$, $McCO_3$, and MgO. La_2O_3 was obtained from Péchiney, and 3*n* Ga_2O_3 from Alusuisse. Host lattice formation was achieved after $2 \times 2\ h$ at 1400°C and checked with X-ray diagrams. Reduction of Mn was carried out at 1300°C in N_2 with a few percent of H_2. The amount of Mn ranged between 0.1 and 2 at.%. Unless otherwise stated, the results presented here were obtained from samples with 0.3–0.4 at.%, which showed highest efficiency. The performance of the standard optical measurements was described previously (*4*). It was difficult to measure reliable excitation spectra in the region 200–300 nm, owing to slow buildup of the luminescence. Increasing the excitation intensity helped to overcome this. Mn^{2+} excitation bands at wavelengths $\geqq 400$ nm were obtained with a Hitachi grating IR spectrophotometer, using KBr and CsBr pellets and paraffin, for the frequency regions of, respectively, 4000–400, 700–200, and 200–70 cm^{-1}.

Results and Discussion

Crystal Structure of the Host Lattices

The unit cells of the hexagonal magnetoplumbite contain spinel blocks, which form plates perpendicular to the threefold axis. The plates are connected by layers of deviating structure, containing the large positive ions (*5*). It is assumed that Mn^{2+} ($r_{Mn} \approx 0.80$ Å) replaces Ga^{3+} ($r_{Ga} \approx 0.62$ Å) or Mg^{2+} ($r_{Mg} \approx 0.66$ Å) rather than the large cations ($1.02 \leqq r \leqq 1.34$ Å). Per unit cell there are 18 octahedral, 4 tetrahedral, and 2 pentahedral sites occupied by Fe (*6*) or, in our case, Ga. In the section on luminescence evidence will be presented that Mn^{2+} occupies a tetrahedral site. The X-ray powder diagrams of (SrGa), (BaGa), and (LaMg)$Ga_{11}O_{19}$ were indexed and the lattice parameters calculated. In Table I the results are summarized and compared with those for various magnetoplumbites obtained by Adelskjöld (*7*), Townes et al. (*6*) and Kato and Saalfeld (*8*).

$SrGa_{12}O_{19}$ and $LaMgGa_{11}O_{19}$ form solid

TABLE I

LATTICE PARAMETERS AND PROBABLE SPACE GROUP OF VARIOUS MAGNETOPLUMBITES

Lattice	a	c	Probable space group	Ref.
$CaAl_{12}O_{19}$	5.564 ± 0.002	21.892 ± 0.005	$P6_3/mmc$	8
$SrAl_{12}O_{19}$	5.557	21.945		7
$BaAl_{12}O_{19}$	5.577	22.67		7
$SrFe_{12}O_{19}$	5.846	23.03		7
$BaFe_{12}O_{19}$	5.893	23.194		6
$PbFe_{12}O_{19}$	5.877	23.02	$P6_3/mmc$	7
$SrGa_{12}O_{19}$	5.796 ± 0.004	22.84 ± 0.02	$P6_3/mmc$	This work
$BaGa_{12}O_{19}$	5.850 ± 0.004	23.77 ± 0.02	?	This work
$LaMgGa_{11}O_{19}$	5.799 ± 0.003	22.71 ± 0.01	$P6_3/mmc$	This work

solutions throughout the whole concentration range. There is extensive solubility of $BaGa_{12}O_{19}$ in $SrGa_{12}O_{19}$, but at $Ba > 0.8$, phase separation occurs. All gallates show reflections (h,h,l) with $h \neq 0$ only when $l = 2n$. Reflections $(0,0,l)$ of $BaGa_{12}O_{19}$ appear also with some values of $l =$ odd, those of $SrGa_{12}O_{19}$ and $LaMgGa_{11}O_{19}$ only with $l = 2n$. The spatial arrangement of the atoms in the $BaGa_{12}O_{19}$ unit cell seems to differ from that in the other gallates. We could not synthesize $CaGa_{12}O_{19}$. The corresponding aluminate exists, the ferrite $CaFe_{12}O_{19}$ does not (7). Apparently, Ca is too small to stabilize a lattice with relatively large tervalent cations such as Ga and Fe. We did, however, synthesize a magnetoplumbite with the composition $CaAl_6Ga_6O_{19}$.

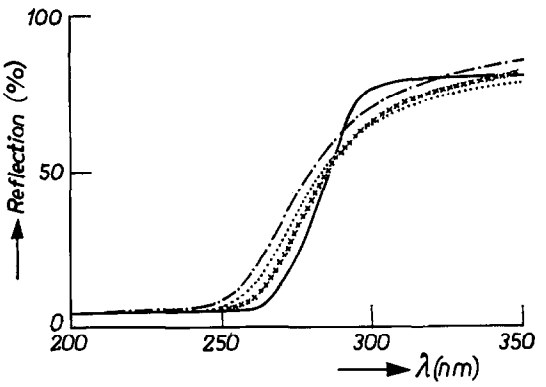

FIG. 1. Diffuse reflection spectra of Sr (drawn curve), $Sr_{0.75}La_{0.25}$ (crossed curve), $Sr_{0.50}La_{0.50}$ (dotted curve), and La (dashed—dotted curve.)

Luminescence

The Host Lattices

Throughout this paper mixed crystals of $SrGa_{12}O_{19}$ and $LaMgGa_{11}O_{19}$ play an important role. For convenience we introduce the following abbreviations: Sr, $Sr_{0.75}La_{0.25}$, $Sr_{0.50}La_{0.50}$, $Sr_{0.25}La_{0.75}$, La, and Ba for $SrGa_{12}O_{19}$, $Sr_{0.75}La_{0.25}Mg_{0.25}Ga_{11.75}O_{19}$, $Sr_{0.50}La_{0.50}Mg_{0.50}Ga_{11.50}O_{19}$, $Sr_{0.25}La_{0.75}Mg_{0.75}Ga_{11.25}O_{19}$, $LaMgGa_{11}O_{19}$, and $BaGa_{12}O_{19}$, respectively. Figure 1 shows diffuse reflection curves of Sr, $Sr_{0.75}La_{0.25}$, $Sr_{0.50}La_{0.50}$, and La. Two effects are noteworthy. (i) The absorption edge shifts to shorter wavelengths when LaMg replaces SrGa; and (ii) the absorption edge of Sr is notably steeper and is crossed over by that of $Sr_{0.75}La_{0.25}$, $Sr_{0.50}La_{0.50}$, and La. The non-activated host lattices luminesce weakly at room temperature but relatively strong at 77°K. Relevant data concerning the host lattice absorption and emission are shown in Table II.

Activation with Mn^{2+}

Figure 2 shows the excitation (Mn^{2+} emission) and diffuse reflection spectra of Sr, $Sr_{0.75}La_{0.25}$, La, and Ba, activated with Mn^{2+}. The spectra of $Sr_{0.50}La_{0.50}$, which do not deviate from the pattern, have been omitted for clarity. Excitation bands of Mn^{2+} in $BaGa_{12}O_{19}$ and $SrGa_{12}O_{19}$ between 350 and 500 nm are given in Table III. They are assigned and complemented with those given by Palumbo for $MgGa_2O_4$:Mn (9).

The $^4T_{1g}$ level in all our phosphors was obscured by the emission band. This points to a Stokes shift of ≤ 20 nm (800 cm^{-1}), comparable

TABLE II

DATA OF THE HOST LATTICE ABSORPTION AND EMISSION IN NONACTIVATED AND Mn^{2+}-ACTIVATED GALLATES

Host lattices	Nonactivated host lattices			Mn^{2+}-activated host lattices		
	Abs. edge at 300°K (cm^{-1})[a]	Emission max. at 77°K (cm^{-1})	T_{50}[b] (°K)	Abs. edge at 300°K (cm^{-1})[a]	Emission max. at 77°K (cm^{-1})	T_{50}[b] (°K)
Sr	37.400	22.170	200	36.950	21.880	145
$Sr_{0.75}La_{0.25}$	38.180	22.270	220	37.450	22.080	210
$Sr_{0.50}La_{0.50}$	38.940	23.310	250	38.200	22.320	250
La	39.600	23.590	265	38.800	24.510	270

[a] Value at 10% reflection.

[b] T_{50} is the temperature in °K at which 50% of the maximum brightness has been quenched.

to that in ZnS and ZnSe:Mn (*10*, *11*). From the data in Table III, v. Gorkom of Philips Research Laboratories calculated a crystal field parameter *Dq* of about 520 cm^{-1}, equal to that found by Palumbo for $MgGa_2O_4$:Mn (*9*). The close similarity of the Mn^{2+} excitation bands in the spinel and magnetoplumbites strongly points to a similar site symmetry of Mn^{2+} in both structures. This rules out the pentahedral site as being occupied by manganese in the magnetoplumbites; these sites would also show a completely different splitting of the Mn^{2+} ^4G level. The order of magnitude of *Dq* indicates tetrahedral surrounding of the Mn^{2+} ion. This was confirmed by measurements of the decay of the Mn^{2+} emission. We found 5 msec close to the calculated value of 2–3 msec in a tetrahedral field (12), a value corresponding to measurements with ZnS:Mn (*13*). The decay of the emission of octahedrally surrounded Mn^{2+} is in general 15–20 msec.

Figure 3 shows the emission curves of Sr:Mn with various Mn^{2+} concentrations at 77°K.

TABLE III

POSITION AND ASSIGNMENT OF EXCITATION BANDS OF Mn^{2+} IN MAGNETOPLUMBITES AND $MgGa_2O_4$. "—" MEANS: NOT LOOKED FOR

Lattice	Assignment	Position at 77°K (nm)	Position at 77°K (cm^{-1})	Position at 300°K (nm)	Position at 300°K (cm^{-1})	Ref.
Sr	$^4T_{1g}(^4G)$	Not observed		Not observed		This work
	$^4T_{2g}(^4G)$	447	22.380	447	22.370	
	^4E_g–$^4A_{1g}(^4G)$	425	23.560	425	23.550	
	$^4T_{2g}(^4D)$	—	—	—	—	
Ba	$^4T_{1g}(^4G)$	Not observed		Not observed		This work
	$^4T_{2g}(^4G)$	449	22.300	448	22.330	
	^4E_g–$^4A_{1g}(^4G)$	425	23.520	426	23.460	
	$^4T_{2g}(^4D)$	—	—	382	26.180	
$MgGa_2O_4$	$^4T_{1g}(^4G)$	479	20.890	—	—	*9*
	$^4T_{2g}(^4G)$	447	22.380	—	—	
	^4E_g–$^4A_{1g}(^4G)$	424	23.580	—	—	
	$^4T_{2g}(^4D)$	380	26.320	—	—	

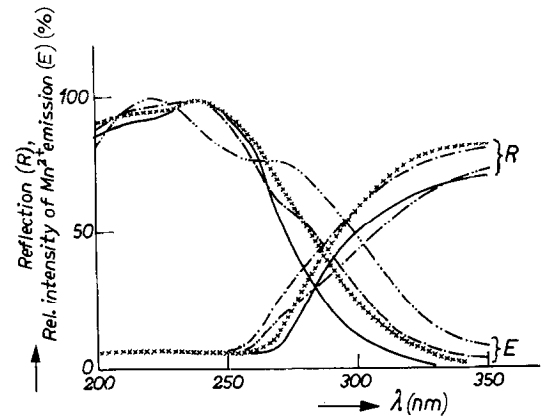

FIG. 2. Relative excitation spectra of the Mn^{2+} emission (E) and diffuse reflection spectra (R) of Sr:Mn (drawn curve), $Sr_{0.75}La_{0.25}$:Mn (crossed curve), La:Mn (—·— curve), and Ba:Mn (—··— curve).

The narrow band at 500 nm is ascribed to Mn^{2+} emission, the broad one at about 450 nm to host lattice emission. The figure is drawn in such a way that the Mn^{2+} emission band peaks at the same height. Integration under the emission curves shows us that the total quantum efficiency remains approximately the same, but the quantum efficiency of the Mn^{2+} emission increases at the expense of that of the host lattice emission, indicating efficient energy transfer. At the optimum Mn^{2+} concentration (0.3%) the host lattice emission of Sr:Mn is quenched at 200°K. However, the Mn^{2+} emission reaches its maximum quantum efficiency at approximately 300°K. The same holds for $Sr_{0.75}La_{0.25}$:Mn, $Sr_{0.50}La_{0.50}$:Mn, $Sr_{0.25}La_{0.75}$:Mn, and La:Mn, but at higher temperature. Table IV gives the maximum quantum efficiencies of the Mn^{2+} emission (qe_m) and the temperature T_m at which this qe_m is reached for the various magnetoplumbites. The energy transfer in Ba:Mn was inefficient in all temperature regions.

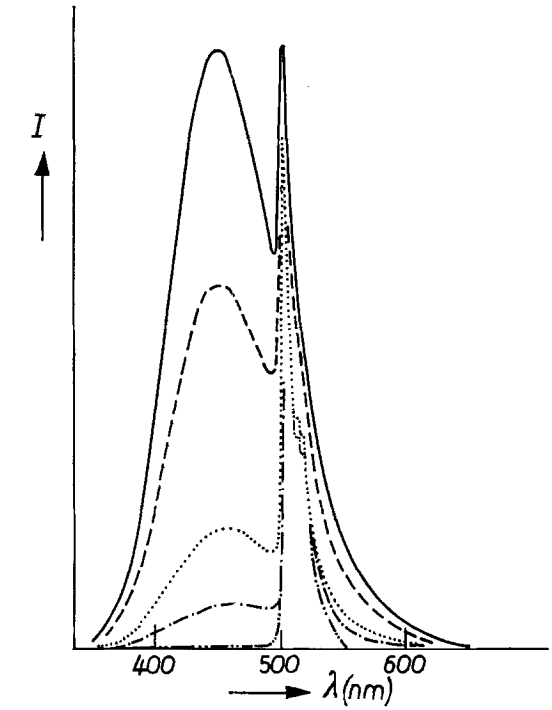

FIG. 3. Spectral energy distribution at 77°K of Sr, activated with 0.1 at.% Mn (drawn curve), with 0.2 at.% Mn (dashed curve), with 0.5 at.% Mn (dotted curve), with 1 at.% Mn (—·— curve), and with 2 at.% Mn (—··— curve). I gives the radiant power per constant wavelength interval in arbitrary units. Excitation with 254 nm radiation.

TABLE IV

MAXIMUM QUANTUM EFFICIENCIES (qe_m) OF THE Mn^{2+} EMISSION AND THE TEMPERATURES (T_m) IN °K AT WHICH THIS qe_m IS REACHED IN VARIOUS MAGNETOPLUMBITES

Host lattice	qe_m (%)	T_m (°K)
Sr	65	300
$Sr_{0.75}La_{0.25}$	65	330
$Sr_{0.50}La_{0.50}$	65	360
$Sr_{0.25}La_{0.75}$	70	365
La	55	370
Ba	15	~300

The increase in the Mn^{2+} emission after quenching of the host lattice emission can be explained as follows. When the lattice has been excited, the excitation energy may disappear by: (i) emission of host lattice luminescence; (ii) radiationless dissipation; and (iii) transfer to another ion (*14*). Only (iii) may give rise to Mn^{2+} emission. At each temperature there will be equilibrium between the three processes. Apparently at low temperature (i) dominates but at high temperatures (iii), whereas (ii) remains small, as shown by the high quantum efficiencies of many of the phosphors.

Except for the green emission observed when Mn^{2+} is introduced, we also found a red shift Δ of the absorption edge. Δ increases when LaMg replaces SrGa and can be calculated from the values in Table II. The results are summarized in Table V.

TABLE V

RED SHIFT Δ OF THE ABSORPTION EDGE (IN cm^{-1}) OF VARIOUS MAGNETOPLUMBITES OWING TO ACTIVATION BY Mn^{2+}

Host lattice	Δ (cm^{-1})
Sr	450
$Sr_{0.75}La_{0.25}$	630
$Sr_{0.50}La_{0.50}$	740
La	800

Complete understanding of the phenomena requires work on single crystals, which we do not intend to execute. The crucial problem remains the nature of the luminescent center in the gallate host lattices. A rather rough experiment in our laboratory did not reveal any photoconduction at room temperature in Mn^{2+}-activated and nonactivated Sr. However, this should not be put forward as conclusive evidence against a ZnS mechanism. We may draw attention to the fact that the narrow band green Mn^{2+} emission can efficiently be generated by sensitizers of unsuspectedly characteristic nature (*15*).

Fine Structure of the Mn^{2+} Emission

The Mn^{2+} emission band in Sr:Mn and Ba:Mn shows a fine structure at 77°K (Fig. 4). Shoulders (Sr) or a side band (Ba) are found on the red side of the emission bands. This fine structure cannot be attributed to splitting of the $^6A_1$ ground state of Mn^{2+}. A splitting of the $^4T_{1g}$ excited state, as large as 90 cm^{-1} and more, is unlikely. Moreover, one would expect the red side of the emission band to increase in intensity when the temperature is decreased. Therefore the structure is best described as owing to coupling of the electronic transitions with phonons. The far infrared spectra support this. Table VI summarizes the frequencies of the main emission line and its shoulders or side band in cm^{-1}, as they are found at 77°K.

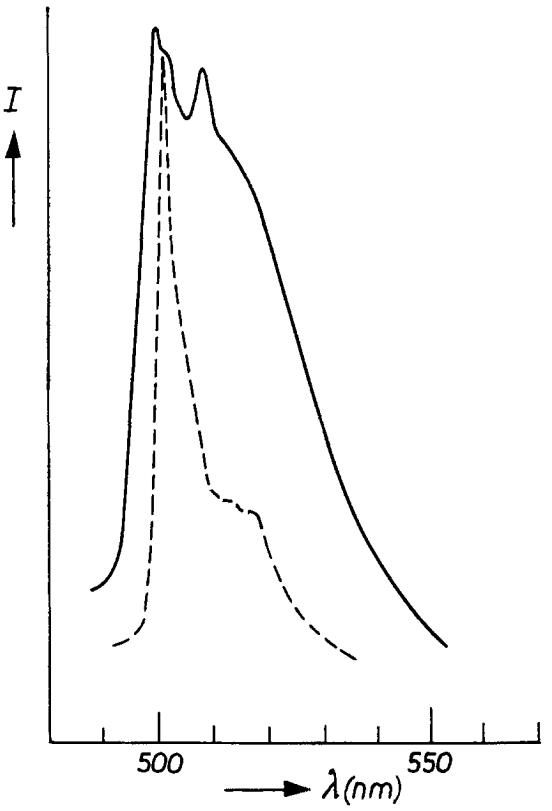

FIG. 4. Fine structure of the Mn^{2+} emission band at 77°K in Ba:Mn (drawn curve) and Sr:Mn (dashed curve). I gives the radiant power per constant wavelength interval in arbitrary units. Excitation with 254 nm radiation.

TABLE VI

POSITION OF MAIN Mn^{2+} EMISSION AND SHOULDERS (SIDE BAND) AT 77°K. FREQUENCIES IN cm^{-1}

Host lattice	Main line (cm^{-1})	Shoulders/side band
Sr	20.000	19.920 (sh), 19.570 (sh), 19.380 (sh)
Ba	20.040	19.720 (side band)

The far infrared spectra show frequencies corresponding to the fine structure. In Sr the strongest absorptions are found at 90, 480, and 650 cm^{-1}, closely fitting the shoulders at 19.920, 19.570, and 19.380 cm^{-1}. The complicated spectrum of Ba shows a defined band at approximately 300 cm^{-1}, corresponding to the side band at 19.720 cm^{-1}.

Acknowledgments

The author gratefully acknowledges fruitful discussions with Mr. Sommerdijk, Mr. Van Gorkom, and Mr. Seuter. Thanks are due also to Mr. J. G. Verlijsdonk, who prepared the samples, and to Dr A. Bril, Mr. J. H. Haanstra, and Mr. C. Bakker for the measurements.

References

1. F. A. KRÖGER, "Some aspects of the luminescence of solids," Elsevier, New York (1948).
2. J. J. BROWN, *J. Electrochem. Soc.* **114**, 245 (1967).
3. W. L. WANMAKER, J. W. TER VRUGT, AND J. G. VERLIJSDONK, *Philips Res. Repts* **25**, 108 (1970).
4. A. BRIL AND W. L. WANMAKER, *J. Electrochem. Soc.* **111**, 1363 (1964).
5. P. B. BRAUN, *Philips Res. Repts* **12**, 491 (1957).
6. W. D. TOWNES, J. H. FANG, AND A. J. PERROTTA, *Z. für Kristallographie* **125**, 437–449 (1967).
7. V. ADELSKJÖLD, *Ark. Kem. Mineralog. Ged. Ser. A***12** **29**, 1–9 (1938).
8. K. KATO AND H. SAALFLED, *Neues Jahrbuch Mineral. Abh.* **109**, 192 (1968).
9. D. T. PALUMBO, *J. Electrochem. Soc.* **117**, 1184 (1970).
10. D. W. LANGER AND S. IBUKI, *Phys. Rev.* **138**, A809 (1965).
11. D. W. LANGER AND H. J. RICHTER, *Phys. Rev.* **146**, 554 (1966).
12. W. E. HAGSTON, *Proc. Phys. Soc.* **92**, 1096 (1967).
13. G. F. J. GARLICK, "Luminescent materials," Oxford U. P., London (1949).
14. TH. P. J. BOTDEN, *Philips Res. Repts* **6**, 425 (1951).
15. J. M. P. J. VERSTEGEN, to be published.